Heterogeneous Catalysis

DOI: 10.1002/anie.201203675

Ceria in Hydrogenation Catalysis: High Selectivity in the Conversion of Alkynes to Olefins**

*Gianvito Vilé, Blaise Bridier, Jonas Wichert, and Javier Pérez-Ramírez**

In recent years, ceria has attracted increasing interest in the fields of medicine, electronics, and chemistry.[1] Its success in catalysis relates to the unique redox and structural properties associated with oxygen diffusion and oxygen storage/release capacity.[2] Because of these intrinsic features, the presence of CeO_2 in combination with noble metals (e.g. Pt and Rh) and other oxides (e.g. γ-Al_2O_3) leads to superior activity and/or lifetime, like in the three-way catalyst for automotive emission control.[3] Additional examples that boosted the use of ceria as a catalyst carrier are 1) the water-gas shift reaction for H_2 generation over La_2O_3-doped Au/CeO_2, 2) the preferential oxidation of CO in H_2-rich streams over Pt or Au/CeO_2, 3) the combustion of alkanes over Cu-promoted CeO_2, and 4) the hydrogenation of different functional groups over CeO_2-supported Ni, Pd, Pt, and Au catalysts.[4] Doped with Gd, Sm, or Au, ceria has been recently applied in the solar-driven thermochemical dissociation of H_2O, while in the pyrolysis of glucose, the addition of CeO_2 to H-ZSM-5 catalysts reduces the formation of coke and enhances the selectivity to acetaldehyde.[5]

Most of the times, ceria does not possess a stand-alone catalytic function, but it magnifies the performance of the main active phase acting as a promoter, stabilizer, or co-catalyst. In fact, the use of pure ceria in heterogeneous catalysis is sporadic and exclusive for oxidations.[6] In hydrogenation catalysis, reduced metals are prototypically applied.[7] Exceptionally, early studies reported that ZnO, ZnO-MnO_2, V_2O_5-Al_2O_3, and Cr_2O_3 are active for the gas-phase hydrogenation of various substrates (e.g. acetonitrile, nitrobenzene, 1-decanol, propene, 1-hexene, 1-octene, butadiene, and acetylene),[8] although selectivity values were often not provided. Density functional theory (DFT) simulations have shown that H_2 adsorbs dissociatively on CeO_2(111) with a relatively low activation barrier (0.2 eV) and strong exothermicity (−2.82 eV),[9] providing strong hints of its potential catalytic function in hydrogenation reactions. CeO_2 and other reducible oxides catalyze the liquid-phase hydrogenation of benzoic acid to benzaldehyde,[10] but other functional groups have not been investigated.

Herein, we report for the first time the catalytic performance of CeO_2 for the partial hydrogenation of alkynes to olefins. This type of reaction, widely exploited in steam crackers for purification of olefin streams as well as in the manufacture of fine chemicals, is conventionally carried out over promoted palladium-based catalysts.[11] In this work, ceria was tested in the gas-phase hydrogenation of propyne (ethyne) at ambient pressure, attaining an olefin selectivity of 91 % (81 %) at a degree of alkyne conversion of 96 % (86 %). We show that the specific surface area and the degree of reduction are key descriptors of the catalytic performance. Operando infrared spectroscopic studies enable to derive a reaction mechanism.

CeO_2 was the sole crystalline phase in the X-ray diffraction pattern of the commercial ceria nanopowder (Figure S1 in the Supporting Information). Chemical composition analyses by inductively coupled plasma optical emission spectroscopy (ICP-OES) corroborated the high purity of the sample, which contains no trace of any conventional hydrogenation metal, such as Pd, Pt, Au, and Ni. The first step was to identify reaction conditions in which CeO_2, calcined at 673 K, was active and selective for propyne hydrogenation. Figure 1 a shows the influence of temperature on the hydrogenation performance, keeping the feed H_2/alkyne ratio and the contact time constant. The propyne conversion is maximal (96 %) at 523 K, with a selectivity to propene of 91 %. The lower conversion above 523 K relates to the detrimental effect of CeO_2 reduction, which starts at about 573 K (Figure S2). This important point is elaborated below. The propene selectivity strongly decreases with temperature, too, from 91 % at 523 K to 25 % at 673 K. Instead, the amount of propadiene formed (propyne isomerization product) increases sharply. Despite the large hydrogen excess in the feed (H_2/C_3H_4 ratio of 30:1), propane formation was not detected at any condition and the selectivity to oligomers was remarkably low (2–10 %). Figure 1 b shows the influence of the feed H_2/C_3H_4 ratio on the activity and the product distribution of CeO_2. The conversion of propyne increases quasi-linearly upon increasing the inlet partial pressure of hydrogen. The selectivity to propene increases, too, while the amount of propadiene progressively drops till zero at a H_2/C_3H_4 ratio of 30:1. These results strongly suggest that hydrogen activation on the ceria surface is the rate-limiting step. To obtain a suitable H coverage for the reaction to proceed selectively on CeO_2, a high hydrogen excess in the feed mixture is required. Otherwise, the hydrogenation activity vanishes and, favored by the high operating temperature, the isomerization of the triple bond to the diene becomes the main process. The selectivity to oligomers did not exceed 10 % even at a H_2/C_3H_4 ratio of 5:1. The effect of

[*] G. Vilé, Dr. B. Bridier, J. Wichert, Prof. J. Pérez-Ramírez
Institute for Chemical and Bioengineering
Department of Chemistry and Applied Biosciences, ETH Zurich
Wolfgang-Pauli-Strasse 10, 8093 Zurich (Switzerland)
E-mail: jpr@chem.ethz.ch

[**] The ETH Zurich is acknowledged for financial support. Dr. C. Mondelli is thanked for discussions on the infrared spectroscopy results.

Supporting information for this article is available on the WWW under http://dx.doi.org/10.1002/anie.201203675.

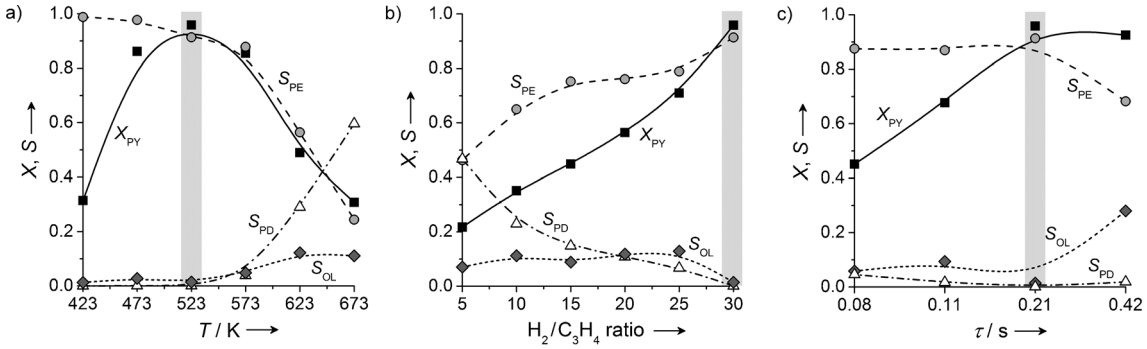

Figure 1. Steady-state conversion of propyne (X_{PY}) and selectivity to propene (S_{PE}), propadiene (S_{PD}), and oligomers (S_{OL}) at 1 bar over CeO_2 versus a) temperature (at a H_2/C_3H_4 ratio of 30:1 and $\tau = 0.21$ s), b) H_2/C_3H_4 ratio (at $T = 523$ K and $\tau = 0.21$ s), and c) contact time (at a H_2/C_3H_4 ratio of 30:1 and $T = 523$ K). Optimal conditions are emphasized.

the contact time is shown in Figure 1c. The propyne conversion doubles when the contact time increases from 0.08 to 0.21 s, while the propene selectivity is practically unchanged. However, a longer contact time favors C–C coupling reactions (selectivity to oligomers up to 27%) at the expense of a lower olefin yield. As a control experiment, we assessed the sensitivity of the reaction selectivity to metal impurities. For this purpose, we deposited minute amounts of palladium (0.05 wt% Pd) on CeO_2 and evaluated the performance in propyne hydrogenation, under the optimal conditions identified for ceria. As shown in Figure S3, the undesired fully hydrogenated product (propane) was obtained with a selectivity exceeding 95%.

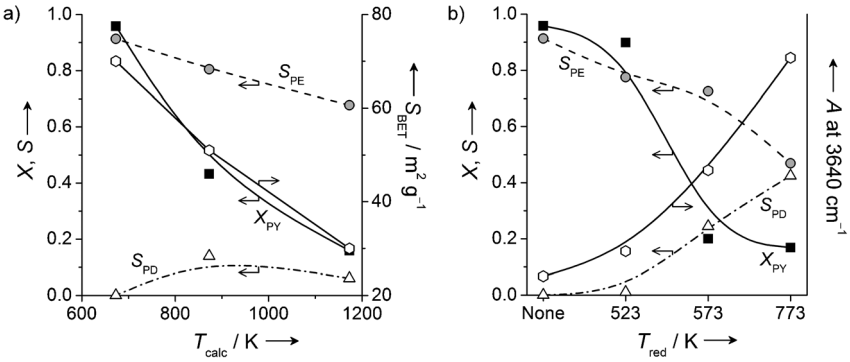

Figure 2. Conversion of propyne (X_{PY}) and selectivity to propene (S_{PE}) and propadiene (S_{PD}) at 1 bar as a function of a) the calcination temperature and b) the reduction temperature of CeO_2. Reaction conditions: H_2/C_3H_4 ratio of 30:1, $T = 523$ K, and $\tau = 0.21$ s. The influence of the calcination temperature on the specific surface area of the solid (S_{BET}; determined by N_2 sorption) and the reduction temperature on the extent of surface vacancies (determined by infrared spectroscopy; A = absorbance) are plotted in the secondary y axis of (a) and (b), respectively.

The unprecedented selective character of CeO_2 for partial alkyne hydrogenation was corroborated using ethyne as the substrate. In this case, a stable selectivity to ethene of 81% at an ethyne conversion of 86% was achieved at 523 K, a H_2/C_2H_2 ratio of 30:1, and $\tau = 0.35$ s. These results exceed the performance of conventional metal-based catalysts,[11] implying promising perspectives for application in hydrorefining of C_2–C_3 cuts in steam crackers. It should be stressed that all the catalytic data reported here were measured under steady-state conditions, and that the performance was stable at every condition for at least 4 h. Other reducible metal oxides, specifically TiO_2, ZnO, and V_2O_5, were evaluated in propyne/ethyne hydrogenation at the above conditions. These oxides were inactive, further emphasizing the outstanding properties of CeO_2. In the literature,[8b] V_2O_5 was reported to hydrogenate ethyne at 673 K with a selectivity to ethane of 93%, although other conditions were not stated.

A high specific surface area and a controlled degree of surface reduction are crucial features for CeO_2 to perform as a superior hydrogenation catalyst. Figure 2a illustrates that the propyne conversion (strongly) and the propene selectivity (moderately) decrease upon increasing the calcination temperature of the sample. This relates well to the decreased specific surface area of CeO_2 at a higher calcination temperature because of sintering. This was substantiated by H_2 temperature-programmed reduction (H_2-TPR, Figure S4) and TEM (Figure S5) analyses. Figure 2b displays the influence of the degree of surface reduction on the catalytic performance. The highest propyne conversion and propene selectivity were obtained with the oxidic catalyst. Upon pre-reduction of CeO_2 in 5 vol% H_2/He (see H_2-TPR in Figure S2), the alkyne conversion and alkene selectivity decreased drastically. The effect is more pronounced at a higher reduction temperature, and has been correlated with a gradual increase of surface vacancies detected by infrared spectroscopy (absorption at 3640 cm^{-1}).[12c] This result, consistent with the decreased propyne conversion above 573 K in Figure 1a, points to the detrimental influence of surface reduction (directly linked to the amount of vacancies) on the catalytic efficiency. This contrasts with the beneficial role of oxygen vacancies on CeO_2 in oxidations and

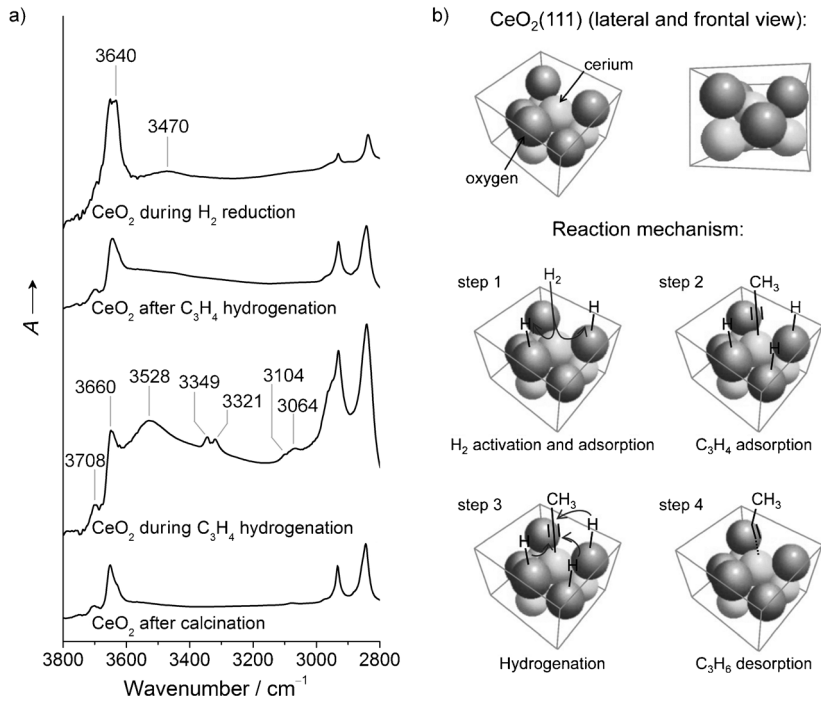

Figure 3. a) DRIFT spectra of CeO_2 recorded at 523 K, after calcination (in He flow), during hydrogenation of propyne (H_2/C_3H_4 ratio of 30:1 and $\tau = 0.21$ s), after hydrogenation of propyne (in He flow), and during reduction of H_2 (in 5 vol% H_2/He; A = absorbance). b) Lateral and frontal views of the $CeO_2(111)$ facet depicting the proposed reaction mechanism.

water-gas shift reactions,[4e,6] pointing to differing criteria in the design of ceria as oxidation or hydrogenation catalyst.

Further understanding of the reaction mechanism was gathered by operando infrared spectroscopy, which is complemented by published DFT simulations.[9] Figure 3b schematically shows the different steps involved in the reaction. Hydrogen dissociatively adsorbs on surface oxygen, leading to two OH groups (step 1). Comparing the spectra of the calcined catalyst with the one recorded under reaction conditions (Figure 3a), an increase in the OH stretching region bands was observed. In particular, the bands at 3708 and 3660 cm^{-1} are assigned to mono-coordinated and doubly bridging OH species.[12c] The broad OH absorption at 3528 cm^{-1} appeared only in the presence of C_3H_4 and relates to the hydrogen abstraction from propyne, which forms another hydroxy group.[12b] This abstraction is favored by the strong acidic/basic sites of ceria (cerium and oxygen atoms, respectively),[12a] and leads to the formation of methylacetylide ($CH_3{-}C{\equiv}C$) onto the cerium atom (step 2). A similar behavior was reported for the interaction of other hydrocarbon molecules with ceria.[2a] Methylacetylide is partially hydrogenated to produce propene (step 3), which finally desorbs as shown in step 4. In fact, the bands at 3104 and 3064 cm^{-1} are due to gas-phase propene.[12d] Adsorbed water, with the characteristic band at 3470 cm^{-1},[12d] was detected during the reduction in H_2 (proving the formation of oxygen vacancies), but not under reaction conditions. After the reaction, all the bands assigned to propyne and propene vanished and a clean surface with the characteristic structural bands of ceria was obtained. The evolution with time of the diffuse reflectance infrared Fourier transform (DRIFT) spectra is displayed in Figure S6. The above-mentioned observations and assignments suggest that surface oxygen species are crucial to stabilize active hydrogen.

A milestone for future studies is to establish the link between oxidation and hydrogenation catalysis over ceria. In oxidations, oxygen vacancies are essential for the performance of ceria and are easier to form on the (100) and (110) facets, while the (111) surface has the less mobile oxygen atoms.[4e] In contrast, our data points to the detrimental influence of an excessive degree of surface reduction on the hydrogenation performance of ceria. Attending to these observations, it can be inferred that the oxygen species involved in hydride transfer might differ from the more mobile oxygen species involved in oxidation reactions. Further studies will focus on studying the gas-phase hydrogenation of alkynes over ceria particles with distinct morphology and thus a variable ratio of exposed planes. In this respect, CeO_2 nanooctrahedra and nanorods with an increased relative amount of (111) and (110) surfaces, respectively, have been reported. Dedicated mechanistic studies on different facets by DFT are also expected to be useful. These studies could also explain the low degree of oligomerization over CeO_2. We tentatively attribute it to the "site isolation" of cerium atoms (each cerium atom is surrounded by four surface oxygen atoms, where hydrogen is adsorbed) in comparison to pure metals, preventing C–C coupling of intermediates and maximizing the olefin production.

In conclusion, we have reported for the first time the superior performance of bulk CeO_2 in the gas-phase hydrogenation of alkynes. With a propene (ethene) selectivity of 91% (81%) at a high degree of alkyne conversion and stable behavior, pure ceria is one of the most efficient catalysts ever reported for this industrially relevant reaction. The high yields have been ascribed to the influence of both the surface area and the degree of surface reduction. The latter, in particular, impacts on the lattice structure through the formation of oxygen vacancies, which are detrimental for the hydrogenation performance. Recent results have confirmed that even the use of ceria supported on an inert carrier, like anatase TiO_2, leads to a high propyne conversion (86%) and propene selectivity (93%), and that the amount of oxygen vacancies of the support is closely connected to the degree of vacancies on the CeO_2 phase and, therefore, to the catalytic performance of the material. This contribution opens exciting perspectives for exploring this oxide as a catalyst for the selective hydrogenation of other functional groups.

Experimental Section

Commercial CeO_2 nanopowder (Aldrich, ref: 1001091023) with a total surface area of 70 $m^2 g^{-1}$ in the as-received form was calcined in static air at different temperatures in the range of 673–1173 K for 5 h using a heating rate of 5 K min^{-1} and eventually in situ pre-reduced in 5 vol% H_2/He at 523–773 K. The gas-phase hydrogenation of ethyne and propyne was studied over these materials at 1 bar in a continuous-flow fixed-bed microreactor (12 mm in diameter) using 0.3 g of the catalyst (particle size = 0.2–0.4 mm) at variable temperatures (423–673 K), contact times (τ = 0.08–0.42 s), and feed H_2/C_3H_4 ratios (5–30). The inlet alkyne concentration was 2.5 vol% and the H_2 concentration was varied using He as the balance gas. The composition of the gas at the reactor outlet was analyzed by an online gas chromatograph (Agilent GC6890N), equipped with a GS-GasPro column, and a flame ionization detector. The conversion of alkyne, *X*, was determined as the amount of reacted alkyne divided by the amount of alkyne at the reactor inlet. The selectivity of each compound, *S*, was calculated as the quantity of product formed divided by the amount of converted alkyne. The selectivity to oligomers was obtained using the carbon balance, $S_{OL} = 1 - \Sigma_i S_i$, in which *i* represents alkanes, alkenes, and alkadienes formed. Other oxides evaluated in alkyne hydrogenation were ZnO (Carl Bittmann, ref: 8849), anatase TiO_2 (Aldrich, ref: 637254), rutile TiO_2 (ABCR, ref: AB204459), and V_2O_5 (Aldrich, ref: 223794). Operando infrared spectroscopy in alkyne hydrogenation was carried out in a Thermo Nicolet 5700 spectrometer equipped with a SpectraTech Collector II diffuse reflectance infrared Fourier transform (DRIFT) accessory and a high-temperature cell, ZnSe windows, and a mercury–cadmium–telluride (MCT) detector. The cell was filled with powdered catalyst and carefully leveled off to reduce reflections of the sample surface and to ensure reproducible results. The spectra were automatically recorded every 10 minutes, in the range of 650–4000 cm^{-1}, by co-addition of 200 scans at a nominal resolution of 4 cm^{-1}. The catalysts prior to and after the reaction were characterized by inductively coupled plasma optical emission spectroscopy (Horiba Ultra 2), X-ray diffraction (PANanalytical X'Pert PRO-MPD), N_2 sorption at 77 K (Quantachrome Quadrasorb-SI), transmission electron microscopy (Phillips CM12), and temperature-programmed reduction of H_2 (Thermo TPDRO 1100).

Received: May 11, 2012
Revised: July 4, 2012
Published online: July 18, 2012

Keywords: alkynes · ceria · heterogeneous catalysis · hydrogenation · olefins

[1] a) E. P. Murray, T. Tsai, S. A. Barnett, *Nature* **1999**, *400*, 649–651; b) J. Chen, S. Patil, S. Seal, J. F. McGinnis, *Nat. Nanotechnol.* **2006**, *1*, 142–150; c) W. C. Chueh, Y. Hao, W. Jung, S. M. Haile, *Nat. Mater.* **2012**, *11*, 155–161.

[2] a) A. Trovarelli, *Catal. Rev. Sci. Eng.* **1996**, *38*, 439–520; b) M. V. Ganduglia-Pirovano, A. Hofmann, J. Sauer, *Surf. Sci. Rep.* **2007**, *62*, 219–270; c) M. V. Ganduglia-Pirovano, J. L. F. Da Silva, J. Sauer, *Phys. Rev. Lett.* **2009**, *102*, 026101; d) J. A. Farmer, C. T. Campbell, *Science* **2010**, *329*, 933–936.

[3] a) A. Trovarelli in *Catalysis by Ceria and Related Materials*, Imperial College Press, London, **2002**; b) R. J. Gorte, *AIChE J.* **2010**, *56*, 1126–1134.

[4] a) Q. Fu, H. Saltsburg, M. Flytzani-Stephanopoulos, *Science* **2003**, *301*, 935–938; b) S. Carrettin, P. Concepción, A. Corma, J. M. López Nieto, V. F. Puntes, *Angew. Chem.* **2004**, *116*, 2592–2594; *Angew. Chem. Int. Ed.* **2004**, *43*, 2538–2540; c) P. Concepción, A. Corma, J. Silvestre-Albero, V. Franco, J. Y. Chane-Ching, *J. Am. Chem. Soc.* **2004**, *126*, 5523–5532; d) J. A. Rodriguez, P. Liu, J. Hrbek, J. Evans, M. Pérez, *Angew. Chem.* **2007**, *119*, 1351–1354; *Angew. Chem. Int. Ed.* **2007**, *46*, 1329–1332; e) R. Si, M. Flytzani-Stephanopoulos, *Angew. Chem.* **2008**, *120*, 2926–2929; *Angew. Chem. Int. Ed.* **2008**, *47*, 2884–2887; f) F. Yang, J. Graciani, J. Evans, P. Liu, J. Hrbek, J. F. Sanz, J. A. Rodriguez, *J. Am. Chem. Soc.* **2011**, *133*, 3444–3451; g) M. Makosch, J. Sa, C. Kartusch, G. Richner, J. A. van Bokhoven, K. Hungerbühler, *ChemCatChem* **2012**, *4*, 59–63.

[5] a) W. C. Chueh, C. Falter, M. Abbott, D. Scipio, P. Furler, S. M. Haile, A. Steinfeld, *Science* **2010**, *330*, 1797–1801; b) A. Primo, T. Marino, A. Corma, R. Molinari, H. García, *J. Am. Chem. Soc.* **2011**, *133*, 6930–6933; c) G. T. Neumann, J. C. Hicks, *ACS Catal.* **2012**, *2*, 642–646.

[6] A. P. Amrute, C. Mondelli, M. Moser, G. Novell-Leruth, N. López, D. Rosenthal, R. Farra, M. E. Schuster, D. Teschner, T. Schmidt, J. Pérez-Ramírez, *J. Catal.* **2012**, *286*, 287–297.

[7] S. Nishimura in *Handbook of Heterogeneous Catalytic Hydrogenation for Organic Synthesis*, Wiley, New York, **2001**.

[8] a) P. Sabatier, A. Fernandez, *Compt. Rend.* **1927**, *185*, 241–244; b) V. I. Komarewsky, L. B. Bos, J. R. Coley, *J. Am. Chem. Soc.* **1948**, *70*, 428–430; c) V. I. Komarewsky, D. Miller, *Adv. Catal.* **1957**, *9*, 707–715.

[9] a) K. Sohlberg, S. T. Pantelides, S. J. Pennycook, *J. Am. Chem. Soc.* **2001**, *123*, 6609–6611; b) G. Vicario, G. Balducci, S. Fabris, S. de Gironcoli, S. Baroni, *J. Chem. Phys. B* **2006**, *110*, 19380–19385; c) H. T. Chen, Y. M. Choi, M. Liu, M. C. Lin, *ChemPhysChem* **2007**, *8*, 849–855.

[10] D. G. Cheng, M. Chong, F. Chen, X. Zhan, *Catal. Lett.* **2008**, *120*, 82–85.

[11] a) A. Borodziński, G. C. Bond, *Catal. Rev. Sci. Eng.* **2008**, *50*, 379–469; b) D. Teschner, J. Borsodi, A. Wootsch, Z. Révay, M. Hävecker, A. Knop-Gericke, S. D. Jackson, R. Schlögl, *Science* **2008**, *320*, 86–89; c) J. A. Anderson, J. Mellor, R. P. K. Wells, *J. Catal.* **2009**, *261*, 208–216; d) B. Bridier, N. López, J. Pérez-Ramírez, *Dalton Trans.* **2010**, *39*, 8412–8419; e) M. García-Mota, J. Gómez-Díaz, G. Novell-Leruth, C. Vargas-Fuentes, L. Bellarosa, B. Bridier, J. Pérez-Ramírez, N. López, *Theor. Chem. Acc.* **2011**, *128*, 663–673.

[12] a) J. M. Vohs, M. A. Barteau, *J. Phys. Chem.* **1990**, *94*, 882–885; b) V. R. Choudhary, V. H. Rane, *J. Catal.* **1991**, *130*, 411–422; c) A. Badri, C. Binet, J. C. Lavallay, *J. Chem. Soc. Faraday Trans.* **1996**, *92*, 4669–4673; d) B. H. Stuart in *Infrared Spectroscopy—Fundamentals and Applications*, Wiley, Chichester, **2004**.

